

The HARPS search for southern extra-solar planets ★

XXXII. Only 4 planets in the Gl 581 system

T. Forveille^{1,2}, X. Bonfils¹, X. Delfosse¹, R. Alonso³, S. Udry³, F. Bouchy^{4,5}, M. Gillon⁶, C. Lovis³, V. Neves^{1,7,8}, M. Mayor³, F. Pepe³, D. Queloz³, N.C. Santos^{7,8}, D. Ségransan³, J.-M. Almenara^{9,10,11}, H.J. Deeg^{10,11}, and M. Rabus^{10,11,12}

- ¹ UJF-Grenoble 1 / CNRS-INSU, Institut de Planétologie et d'Astrophysique de Grenoble (IPAG) UMR 5274, Grenoble, F-38041, France
² Institute for Astronomy, University of Hawaii, 2680 Woodlawn Drive, Honolulu HI 96822 USA
³ Observatoire de Genève, Université de Genève, 51 ch. des Maillettes, 1290 Sauverny, Switzerland
⁴ Institut d'Astrophysique de Paris, CNRS, Université Pierre et Marie Curie, 98bis Bd Arago, F-75014 Paris, France
⁵ Observatoire de Haute-Provence, CNRS/OAMP, F-04870 St Michel l'Observatoire, France
⁶ Université de Liège, Allée du 6 Aout 17 Sart Tilman, Belgium
⁷ Centro de Astrofísica, Universidade do Porto, Rua das Estrelas, 4150-762 Porto, Portugal
⁸ Departamento de Física e Astronomia, Faculdade de Ciências, Universidade do Porto, Rua das Estrelas, 4150-762 Porto, Portugal
⁹ Laboratoire d'Astrophysique de Marseille, 38 rue Frédéric Joliot-Curie, F-13388 Marseille Cedex 13, France
¹⁰ Instituto de Astrofísica de Canarias, E-38205 La Laguna, Tenerife, Spain
¹¹ Dpto. de Astrofísica, Universidad de La Laguna, 38206 La Laguna, Tenerife, Spain
¹² Departamento de Astronomía y Astrofísica, Pontificia Universidad Católica de Chile, Casilla 306, Santiago 22, Chile

ABSTRACT

The Gl 581 planetary system has generated wide interest, because its 4 planets include both the lowest mass planet known around a main sequence star other than the Sun and the first super-Earth planet in the habitable zone of its star. A recent paper announced the possible discovery of two additional super-Earth planets in that system, one of which would be in the middle of the habitable zone of Gl 581. The statistical significance of those two discoveries has, however, been questioned. We have obtained 121 new radial velocity measurements of Gl 581 with the HARPS spectrograph on the ESO 3.6 m telescope, and analyse those together with our previous 119 measurements of that star to examine these potential additional planets. We find that neither is likely to exist with their proposed parameters. We also obtained photometric observations with the 2.5 m Isaac Newton Telescope during a potential transit of the inner planet, Gl 581e, which had a 5% geometric transit probability. Those observations exclude transits for planet densities under 4 times the Earth density within -0.2σ to $+2.7 \sigma$ of the predicted transit center.

Key words. Stars: individual: Gl 581 – Stars: planetary systems – Stars: late-type – Techniques: radial-velocity

1. Introduction

Amongst the almost 500 planetary systems currently listed in the on-line Exoplanet Encyclopedia¹, Gl 581 occupies a special place in both astronomers' and the public's mind, as it contains the only extrasolar planet(s) of likely rocky composition known in the habitable zone of its star, as well as the lightest extrasolar planet known to this date. We first detected Gl 581b (Bonfils et al. 2005b), a Neptune-mass planet with a 5 days period, based on 20 radial velocity measurements with the HARPS spectrograph on the ESO 3.6 m telescope. Motivated in part by structure in the residuals to the Bonfils et al. (2005b) orbit, we then obtained a further 30 HARPS radial velocity measurements. Those 50 observations detected two additional planets, Gl 581c and Gl 581 d (Udry et al. 2007), with minimum masses of 5 and 8 M_{Earth} and orbital periods of 13 and 84 days. The minimum

masses make rocky compositions most likely for both planets, and the periods respectively locate them at the inner and outer edges of the habitable zone of their M3V host star. With a further 69 HARPS measurements, for a total of 119, we finally identified a fourth planet (Mayor et al. 2009), Gl 581e, with a minimum mass under 2 M_{Earth} and a 3 days orbital period. To this date, Gl 581e remains the lowest mass planet listed in the Exoplanet Encyclopedia. Just as importantly for the present discussion, Mayor et al. (2009) also demonstrated that the 84 days Udry et al. (2007) period for Gl 581d was a one-year alias of its true period, 67 days, marginally changing the mass of the planet but bringing it $\sim 13\%$ closer to the star and further into its habitable zone. Finally, Mayor et al. (2009) demonstrated that stability of Gl 581e against the gravitational influence of the more massive planets requires an inclination of the (assumed coplanar) system above 40 degrees, and therefore that the masses of the planets are at most 1.6 times their minimum values.

Gl 581c initially generated most excitement, since rough equilibrium temperature computations suggested that its surface could harbor liquid water, while surface water on Gl 581d would be frozen (Udry et al. 2007). Accounting for the greenhouse effect of atmospheres on both planets, however, Selsis et al. (2007)

Send offprint requests to: T. Forveille, e-mail: Thierry.Forveille@obs.ujf-grenoble.fr

* Based on observations made with the HARPS instrument on the ESO 3.6-m telescope at La Silla Observatory under program ID 072.C-0488, 180.C-0886, 082.C-0718, and 183.C-0437

¹ <http://exoplanet.eu/>

soon showed that an extremely high albedo would be needed for the surface of Gl 581c to escape water boilout, while realistically high concentrations of atmospheric CO₂ might be sufficient to keep Gl 581d from freezing out. The latter planet is therefore by far the better candidate for habitability, a conclusion only made stronger by the ~25% higher stellar flux at its closer Mayor et al. (2009) orbital distance (e.g. Wordsworth et al. 2011).

Most recently, Vogt et al. (2010) announced the discovery of two additional planets in the Gl 581 system, based on a joint analysis of the 119 Mayor et al. (2009) *HARPS* radial velocities and 122 previously unpublished *Keck HIRES* measurements. The two additional planets, Gl 581f and Gl 581g, would have masses of 7 and 3 Earth masses, and periods of 433 and 33 days. That announcement raised considerable interest, since Gl 581g would, if confirmed, sit in the middle of the habitable zone of the system, when Gl 581d instead is close to the cold edge of that zone. While Gl 581d's habitability depends on a thick enough atmosphere producing both a strong greenhouse effect and a vigorous dayside to nightside circulation, Gl 581g would likely be habitable for a broader range of atmospheric parameters. That planet has therefore already been the focus of significant theoretical habitability work, with uniformly positive conclusions (e.g. Pierrehumbert 2011; von Bloh et al. 2011; Heng & Vogt 2011). The Vogt et al. (2010) 5th and 6th planets however are detected at relatively modest significance level. Both detections have therefore been questioned on purely statistical grounds, first by Andrae et al. (2010), and more recently by Tuomi (2011) and Gregory (2011). Anglada-Escudé & Dawson (2010), on the other hand, conclude with some tentative support for Gl 581f, though none for Gl 581g. Beyond purely statistical considerations, merging datasets from independent instruments or analyses necessarily exposes to some risk of being misled by subtle low-level systematics in one or the other, and more so when none of the individual datasets detects the signal of interest. The two additional planets, and particularly the potentially habitable Gl 581g, have therefore generally been received with as much caution as interest.

As we announced at a conference soon after the Vogt et al. (2010) manuscript first became public (Pepe et al. 2011), we had continued observing Gl 581 after the publication of Mayor et al. (2009). Those continuing observations were motivated largely by the dynamical stability island in the middle of the habitable zone where Vogt et al. (2010) announced their discovery of Gl 581g, together with speculations that planetary systems might be “dynamically full”. At that time, we had obtained ~60 additional *HARPS* measurements and announced that we saw no evidence for either f or g. We have since then observed the Gl 581 system with *HARPS* for one additional year, and have now obtained a total of 121 radial velocity measurements above the 119 discussed in Mayor et al. (2009), again approximately doubling the number of *HARPS* measurements. We present the *HARPS* measurements dataset in Section 2, and discuss in Section 3 the limits which it sets on planets beyond the 4 discussed in Mayor et al. (2009). Additionally, we obtained ground-based photometry, discussed in Section 4, to search for transits of the 3-days Gl 581e.

2. HARPS observations

Table 1 summarizes the stellar parameters of Gl 581, which we discussed at some length in our previous publications (Bonfils et al. 2005a; Udry et al. 2007; Mayor et al. 2009). The most important update over those is that Vogt et al. (2010) used differential photometry to identify the likely rotation period of the star,

Table 1. Observed and inferred stellar parameters for Gl 581

Parameter	Gl 581	Reference
Spectral Type	M3V	Hawley et al. (1996)
V	10.55 ± 0.01	Mermilliod et al. (1997)
B–V	1.60 ± 0.01	Mermilliod et al. (1997)
π [mas]	160.91 ± 2.62	van Leeuwen (2007)
Distance [pc]	6.21 ± 0.10	van Leeuwen (2007)
M_V	11.58 ± 0.03	
K	5.85 ± 0.03	Leggett (1992)
M_K	6.88 ± 0.04	
L_\star [L_\odot]	0.013	Delfosse et al. (1998)
L_x/L_{bol}	$< 5 \cdot 10^{-6}$	Delfosse et al. (1998)
[Fe/H]	-0.22	Schlaufman & Laughlin (2010)
M_\star [M_\odot]	0.31 ± 0.02	Bonfils et al. (2005a)
R_\star [R_\odot]	0.29	Bonfils et al. (2005a)
$v \sin i$ [km s^{-1}]	< 1	Udry et al. (2007)
P_{rot} [days]	94.2 ± 1.0	Vogt et al. (2010)
v_{rot} [km s^{-1}]	0.16	This paper
age [Gyr]	> 2	Bonfils et al. (2005a)

94 days. From that period and the $0.29 R_\odot$ radius of Gl 581, one infers an equatorial rotation velocity of just 0.16 km s^{-1} , well under the 1 km s^{-1} spectroscopic upper limit on $v \sin i$. This reinforces previous conclusions that Gl 581 is a very slow rotator, and is consistent to its belonging to the quietest magnetic activity quartile of the *HARPS* M dwarf sample.

Our observing procedure for Gl 581 is, similarly, presented in some detail in our previous papers, and only summarized here. Briefly, we obtain 15 mn exposures of Gl 581 with *HARPS* (High Accuracy Radial velocity Planet Searcher Mayor et al. 2003), and choose to keep the calibration fiber of the spectrograph dark. While simultaneous exposures of a Thorium-Argon lamp spectrum on that fiber and a stellar spectrum on the object fiber provide best velocity stability for *HARPS* (e.g. Lovis et al. 2006; Mayor et al. 2009), our 15 mn exposures of the V = 10.5 Gl 581 do not reach the sub-m/s stability floor of the spectrograph. We can therefore rely on the excellent instrumental stability (nightly instrumental drifts $< 1 \text{ m s}^{-1}$) of *HARPS* and obtain separate calibration exposures. This produces cleaner stellar spectra, suitable for quantitative spectroscopic analyses. We obtained 121 new *HARPS* measurements, for a total of 240 with the (Mayor et al. 2009) included, with a median S/N ratio of 46 per pixel at 550 nm. After accounting for observational overheads and for the average weather statistics at La Silla observatory, our observational investment on this one system now amounts to approximately 10 nights.

The radial velocities (Table 3, only available electronically) were obtained with the standard *HARPS* data reduction pipeline, based on the cross-correlation with a stellar template and the precise nightly wavelength calibration with ThAr spectra (Lovis & Pepe 2007). For homogeneity, and to benefit from the continuous improvements to the *HARPS* pipeline, all measurements have been reprocessed with its latest version. The velocities listed in Table 3 for the 119 measurements in common with Mayor et al. (2009) therefore differ slightly from the values listed in that paper, though usually by a small fraction of their stated standard errors. The velocities have a median internal error of only 1.15 m s^{-1} , which includes the 0.3 m s^{-1} nightly zero-point calibration uncertainty (Lovis & Pepe 2007), the 0.3 m s^{-1} rms calibration drift during a night, and the photon noise computed from the full Doppler information content of the spectra (Bouchy et al. 2001). The latter dominates the error budget for this moderately faint source.

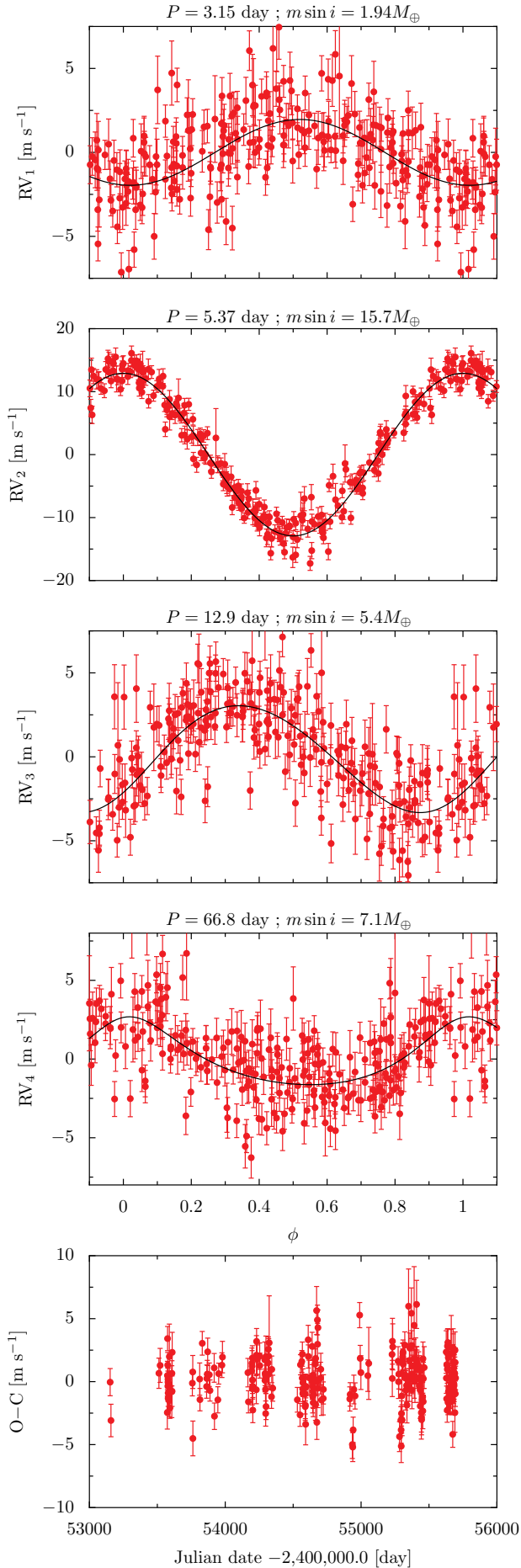


Fig. 1. HARPS radial velocities of Gl 581 phased to the periods of each of Gl 581b to Gl 581e, with the best fits for the other 3 planets subtracted, and residuals to the 4-planets fit as a function of time. The planets are ordered by increasing period (Gl 581e (top), Gl 581b, Gl 581c, Gl 581d, and residuals (bottom). The adjusted Keplerian orbit is overlaid.

3. Orbital analysis

Based on the nominal standard errors of the two datasets, 1.70 m/s for the Vogt et al. (2010) HIRES velocities and 1.15 m/s for our HARPS measurements, the 121 new HARPS measurements have twice the statistical weight of the 122 HIRES velocities which Vogt et al. (2010) analysed together with the 119 Mayor et al. (2009) measurements. Additionally, Gregory (2011) find evidence for ~ 1.8 m/s of additional Gaussian noise ('jitter') above the nominal error bars of the Vogt et al. (2010) HIRES velocities and none for the Mayor et al. (2009). This would reduce the relative information content of the HIRES measurements by another factor of two. Based on their higher statistical weight, and to retain the benefits of a homogeneous dataset, we limit our analysis to the HARPS measurements. One price to pay for this homogeneity is a shorter time span, 7 years instead of 12 years with the HIRES data included. The HARPS measurements however have good phase coverage for both 33 and 433 days periods (Fig. 2), and therefore provide good diagnostic power on their own for Gl 581f and g.

Since all analyses of the Gl 581 system agree on the broad characteristics of planets b to e, we start by adjusting a 4-planets Keplerian orbital model to the HARPS measurements. We then mostly work from its residuals. The resulting orbital model (Table 2, top, and Figure 1) is generally consistent with previous determinations, but has improved errorbars and provides better constrained ephemerides at recent and future dates. The rms amplitude of the residuals from the orbital model is 1.8 m s^{-1} significantly above the 1.15 m s^{-1} average photon noise. The square root of the reduced χ^2 of the fit is consequently 1.6, and the radial velocities thus contain either information beyond the detected planet or excess noise, instrumental or astrophysical. The largest residuals, such as those which stand out at phases 0.5 to 0.6 in the Gl 581b panel of Figure 1, correspond to spectra with low S/N ratio (under 35, compared to a median of 46), obtained through either clouds or degraded seeing. Ignoring those measurements produces visually more pleasing figures, but leaves the orbital parameters essentially unchanged and only modestly lowers the reduced χ^2 of the least square fit. We chose to retain them, for the sake of simplicity.

The adjusted eccentricities are small for all 4 planets, with a formally highest significance of 3.5σ for the 3 days Gl 581e, which is subject to the strongest tidal forces and least expected to have high eccentricity. We therefore experimented with adjusting circular orbits for all 4 planets. The resulting orbital model (Table 2, bottom) has a slightly higher reduced χ^2 , 2.70 compared to 2.57 for the Keplerian model. We adopt the latter as our baseline, but repeated the analyses described below using the residuals of circular orbits, with identical conclusions. The choice is thus of no consequence for the following discussion.

Fig. 2 shows the residuals of the 4-planets Keplerian model phased to the periods of the Vogt et al. (2010) Gl 581f and Gl 581g, as well as the medians of those residuals over 0.05 phase bins. The binned residuals shows no evidence for the ± 1.3 m/s signal expected from the two planets and overlaid as thick curves. To quantify that statement, we adjust a 6-planet model with the the orbital elements of two planets fixed to the Vogt et al. (2010) values for Gl 581f and Gl 581g. That model has a reduced χ^2 of 4.54, well above the 2.57 of the 4-planets model, or equivalently has 75% higher residuals. A 6-planets model with only the periods of Gl 581f and Gl 581g fixed to their Vogt et al. (2010) values does produce a similar reduced χ^2 to the 4-planets model, but it has amplitudes under 40 cm/s for both planets and phases which do not match Vogt et al. (2010)

Table 2. Keplerian (top) and circular (bottom) orbital models of the Gl 581 planetary system.

4 Keplerian orbits				
Parameter	Gl 581 e	Gl 581 b	Gl 581 c	Gl 581 d
P [days]	3.14945 ± 0.00017	5.36865 ± 0.00009	12.9182 ± 0.0022	66.64 ± 0.08
T_0 [JD-2400000]	54750.31 ± 0.13	54753.95 ± 0.39	54763.0 ± 1.6	54805.7 ± 3.4
e	0.32 ± 0.09	0.031 ± 0.014	0.07 ± 0.06	0.25 ± 0.09
ω [deg]	236 ± 17	251 ± 26	235 ± 44	356 ± 19
K [m s ⁻¹]	1.96 ± 0.20	12.65 ± 0.18	3.18 ± 0.18	2.16 ± 0.22
V [km s ⁻¹]		-9.2060 ± 0.0004		
$f(m)$ [$10^{-12} M_\odot$]	0.21	112.46	4.28	6.28
$m \sin i$ [M_\oplus]	1.95	15.86	5.34	6.06
a [AU]	0.028	0.041	0.073	0.22
N_{meas}		240		
Span [days]		2543		
σ (O-C) [ms ⁻¹]		1.79		
χ^2_{red}		2.57		
4 circular orbits				
Parameter	Gl 581 e	Gl 581 b	Gl 581 c	Gl 581 d
P [days]	3.14941 ± 0.00022	5.36864 ± 0.00009	12.9171 ± 0.0022	66.59 ± 0.10
T [JD-2400000]	54748.243 ± 0.056	54750.199 ± 0.012	54761.03 ± 0.11	54806.8 ± 1.0
K [m s ⁻¹]	1.754 ± 0.180	12.72 ± 0.18	3.21 ± 0.18	1.81 ± 0.19
V [km s ⁻¹]		-9.2060 ± 0.0001		
$f(m)$ [$10^{-12} M_\odot$]	0.18	114.54	4.46	4.11
$m \sin i$ [M_\oplus]	1.84	15.96	5.41	5.26
a [AU]	0.028	0.041	0.073	0.22
N_{meas}		240		
Span [days]		2543		
σ (O-C) [ms ⁻¹]		1.86		
χ^2_{red}		2.70		

either. We can therefore safely conclude that the HARPS data excludes Gl 581f and Gl 581g existing with their Vogt et al. (2010) orbital elements.

To investigate planets with potentially somewhat different periods, we turn to a step by step periodogram analysis (Fig. 3), successively removing planets with periods initialized at the highest peak of periodogram of the previous step. To estimate the False Alarm Probability (FAP) of those peaks, we use bootstrap resampling (e.g. Press et al. 1992) of the actual measurements (or residuals) to generate 10,000 virtual datasets, and adopt the fraction of those virtual periodograms with a peak above a given power as the False Alarm Probability for that periodogram power. This bootstrap analysis automatically accounts for the actual level, and the possibly non-Gaussian statistics, of the measurement noise, but not for any correlation between measurement. It can therefore potentially underestimate the actual False Alarm levels. In early iterations the bootstrap analysis on the other hand considers the signal from other planets as noise, and therefore strongly underestimates significance. Fig. 3 displays the periodogram power levels for False Alarm Probabilities equivalent to 1, 2 and 3 σ significance for a Gaussian statistics. The periodogram analysis, unsurprisingly, successively re-identifies Gl 581b to Gl 581e. The highest periodogram peak for the last step (Fig. 3, bottom), which corresponds to the residuals of the 4-Keplerian model, scarcely rises above 1 σ significance. The $\sim 50\%$ excess in the residuals is therefore very unlikely to be explained by one additional planet. It could reflect either astrophysical or instrumental jitter, several planets each contributing a signal below our detection threshold, or a combination thereof.

To evaluate the sensitivity of our dataset to planets with orbital parameters similar to the Vogt et al. (2010) Gl 581f and Gl 581g, we repeat the step by step periodogram analysis for a dataset where we subtract the signatures of those two planets,

with their Vogt et al. (2010) orbital elements, from the HARPS radial velocities (the choice of subtracting, rather than adding, those signatures avoids the suspicion that we could be boosting a pre-existing signal in the HARPS measurement). The last step of that procedure (Fig. 4, second panel from bottom) has a highly significant peak at the period of Gl 581g and a moderately significant one at the period of Gl 581f. Removing the Gl 581g signal brings the False Alarm Probability of the Gl 581f peak down to 0.08% (Fig. 4, bottom panel). This exercise demonstrates that our dataset is sensitive to such planets, and does not find them.

4. Photometric transit search

As mentioned by Mayor et al. (2009), the *a priori* geometric probability that Gl 581e transits across its host star is approximately 5%. Thanks to the small radius of Gl 581, $0.29 R_\odot$, the transit of a 1 Earth radius planet across Gl 581 would induce a 1.1 mmag dip in the observed flux. Non-grazing transits of the 2-Earth-Mass Gl 581e, if they occur at all and unless the planet is much denser than the Earth, would thus be detectable with state of the art ground-based photometry (e.g. Johnson et al. 2009).

We used the WFC camera (Walton et al. 2001) on the 2.5 m Isaac Newton Telescope to observe the potential transit on the night of May 17th to 18th 2009, with a predicted center at JD=2454969.4886 \pm 0.063 (23h43m \pm 1.52 hrs on May 17th 2009). The WFC is a mosaic of 4 2048x4096 EEV CCDs which cover a 34'x34' field of view, with an 11'x11' gap in one corner. The focal scale is 0.333''/pixel. At the time of our observations the detector could neither be binned nor windowed, and the fastest WFC readout time was 29 s. We observed through a Sloan-like r' filter and used 25 s exposures, for a 55 s total inter-exposure time. To avoid saturating the detector, we defocused the telescope to a 15 arcsec image diameter. Since the au-

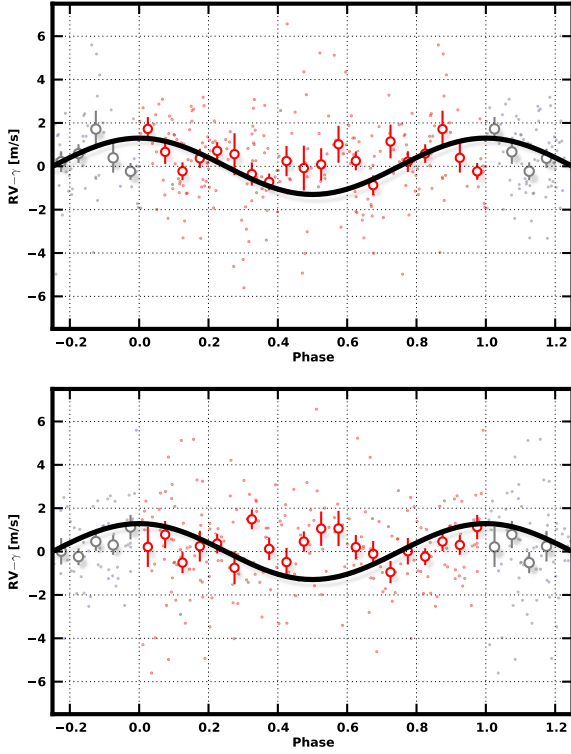


Fig. 2. Residuals of the HARPS radial velocity measurements of Gl 581 to the 4-planets Keplerian model (Table 2), phased to the 433 days period of Gl 581f (top) and to the 36.6 days periods of Gl 581g (bottom). The dots represent the individual residuals, and the open circles their medians over 0.05 phase bins, with vertical errorbars showing the standard error of their mean. The thick curves represent the Vogt et al. (2010) orbits for both planets.

to guiding system of the WFC does not operate on such severely defocused image, the observer guided manually, with measured rms excursions of 1.7 and 2.3 pixels (0.6 and 0.8 arcsec) for the X and Y axes. We obtained flat field exposures on the twilight sky at the end of the night, with the telescope defocused by the same amount as during the observations, and we used a sequence of dome screen exposures with increasing integration times (Gilliland et al. 1993) to verify the linearity of the CCD detectors.

We extracted aperture photometry for the target and several potential reference stars, using a circular aperture of 50 pixel diameter and a sky annulus with 55 and 85 pixels inner and outer diameters. The flux of Gl 581 was then divided by the summed fluxes of 4 bright non variable stars. The resulting light curve (Table 5, only available electronically) shows a low frequency trend, which reflects differential color extinction between the (red) target and its reference stars. That trend is well described by a third order polynomial, which is smooth enough to remove signal on the time-scales of interest for a 1 hour transit only at the edges of the observing window. After dividing out that trend, the lightcurve (Fig. 5) is flat, with a 0.0830% rms scatter and no obvious evidence for a transit. Finally, we mapped the χ^2 residuals of the light-curve with respect to a 1 h long trapeze-shape transit as a function of transit center and depth. At the 4σ confidence level, the resulting map (Figure 6) excludes non-grazing transit deeper than 0.06% within -90 to +210 mn of the predicted transit center. Inserting transits prior to the normalization by the poly-

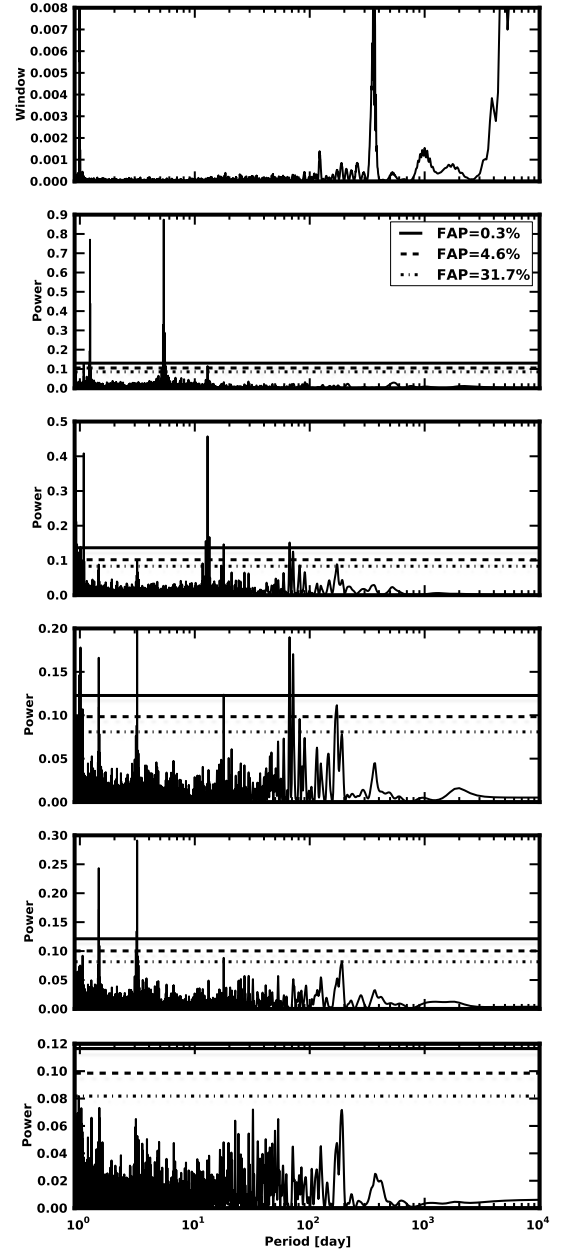


Fig. 3. Periodograms of the HARPS radial velocity measurements of Gl 581, with horizontal lines marking the False Alarm Probabilities corresponding to 1, 2 and 3 σ thresholds for a Gaussian statistics. *Panel 1 (top):* Window function of the measurements *Panel 2:* Periodogram of the HARPS velocities. The peaks corresponding to Gl 581b ($P=5.36d$) and its alias with one sidereal day are prominent, and that for Gl 581c ($P=12.9d$) is easily seen. *Panel 3:* periodogram of the HARPS velocities corrected from the variation due to Gl 581b. The peak corresponding to Gl 581c ($P=12.9d$) becomes prominent, and the peaks corresponding to Gl 581d ($P=67d$) and Gl 581e ($P=3.15d$) and their aliases can be distinguished. *Panel 4:* Removing the variability due to planets b and c makes the peaks due to the $P=3.15d$ Gl 581e (and its alias with the a one sidereal day period) and to the $P=67d$ Gl 581d (and its one year alias). *Panel 5 :* Periodogram after removing the effect of planets b, c and d. The peaks due to Gl 581e (and its one-day aliases) are evident. *Panel 6 (bottom):* Periodogram of the residuals of the 4-planets orbital model, with no additional significant peak.

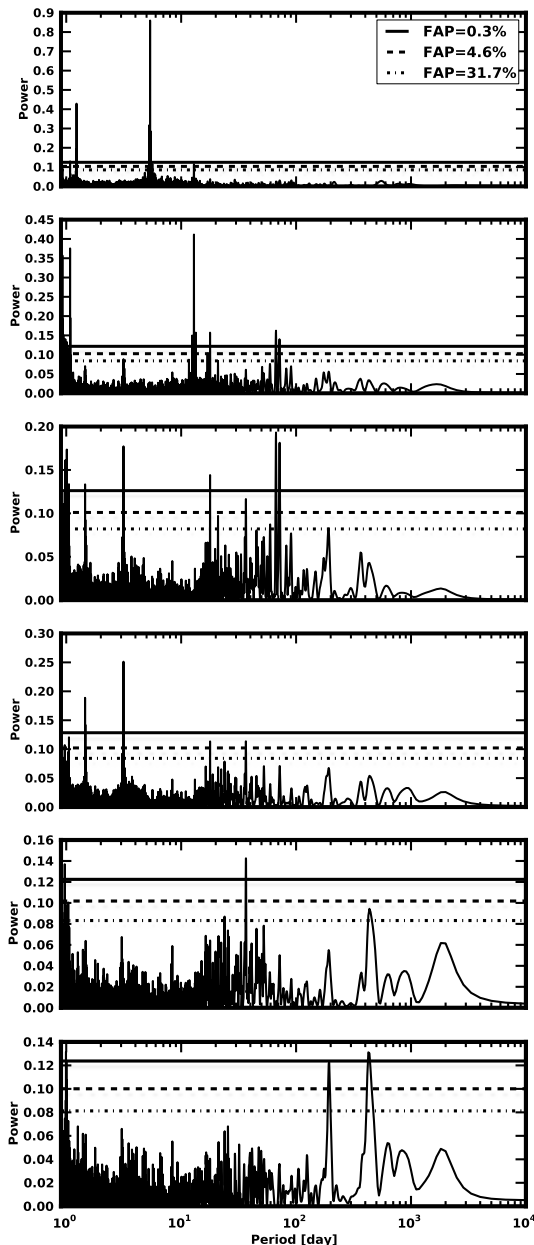


Fig. 4. Equivalent of Fig. 3 for a dataset in which the signatures of Gl 581f and Gl 581g (with their Vogt et al. (2010) orbital elements) are subtracted from the HARPS measurements. The periodogram of the residuals of the 4-planets orbital model has a highly significant peak at the period of Gl 581g and a moderately significant peak at the period of Gl 581f, which becomes significant after subtracting Gl 581g.

nominal baseline however shows that transits in early part of the transit window can be partly absorbed into the polynomial baseline, and that we can exclude 0.06% deep transit only within -20 to $+210$ mn (-0.22 to $+2.5 \sigma$) of the predicted center. This depth translates to a $0.75 R_{\oplus}$ maximum radius, and therefore to a minimum density of 4.4 Earth density, for a non-grazing transiting Gl 581e. The planet is therefore most likely to not transit, but better coverage of the transit window will be needed to fully exclude that it does.

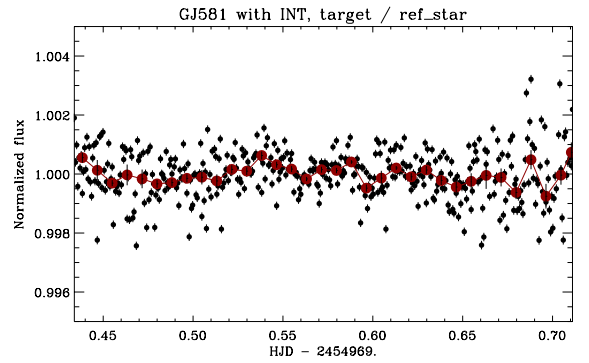


Fig. 5. r' -band differential light curve of Gl 581 during the potential transit of Gl 581e on May 17th 2009, after normalization by a third order polynomial. The light curve shows no evidence for a transit. The black points represent the individual measurements, and the red dots their average over 12 min bins. The dispersion of the black points is 830 ppm, and that of the red points is 342 ppm. For white noise, the expected dispersion of the 12 mn averages would be 230 ppm, revealing 250 ppm of uncorrected systematic red noise on that time-scale.

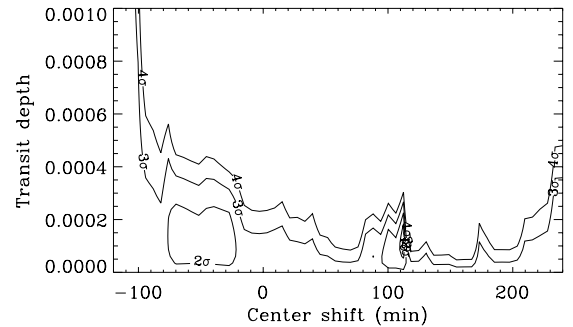


Fig. 6. Map of the χ^2 of the residuals of a fit of a 1 h-long trapeze-shape transit as a function of transit depth and center relative to the predicted time (HJD = 2454969.489).

5. Summary

We observed the Gl 581 planetary system with the HARPS spectrograph for another two years, adding 121 high-quality radial velocity measurements to the 119 which we previously published Mayor et al. (2009). The new measurements refine the parameters of the 4 Mayor et al. (2009) planets, and have in particular revised the minimum mass of Gl 581d down to $6 M_{\text{Earth}}$. The lowered minimum mass of this potentially habitable planet (e.g. Wordsworth et al. 2011) makes a rocky composition more likely. The revised orbital fit also provides a more precise ephemeris for recent and future epochs.

When phased to the Vogt et al. (2010) periods for the candidate Gl 581f and Gl 581g planets, the residuals of the 4-planet orbital fit show no evidence for a coherent signal with the expected 1.2 m/s amplitude. When we add two planets with elements fixed to the Vogt et al. (2010) values for Gl 581f and Gl 581g and readjust the orbital model, its residuals increase by 75%. When instead we fit for two planets with circular orbits of arbitrary amplitude and phase at the periods of Gl 581f and Gl 581g in addition to planets b to e, we obtain amplitudes of 16 and 40 cm/s. In a separate test, we verified that planets with the characteristics of Gl 581f and Gl 581g, but for a π phase shift,

are easily identified in a step by step periodogram analysis. Our dataset therefore has strong diagnostic power for planets with the parameters of Gl 581f and Gl 581g, and we conclude that the Gl 581 system is unlikely to contain planets with those characteristics. This, of course, is not to say that the Gl 581 system can contain no other planet, nor even that it contains no planets with periods close to 33 and 430 days. Both periods correspond to dynamically stable orbits (e.g. Vogt et al. 2010), and planets with similar periods but lower masses or/and different phases certainly could exist under our noise ceiling. Such planets could potentially contribute to the 60% excess of our residuals over our internal errors, together with some combination of astrophysical and instrumental noise. Disentangling those contributions to the excess residuals may however require significant instrumental or methodological improvements, since we already have invested ~10 nights on the Gl 581 system and can no longer easily boost our sensitivity by working up \sqrt{N} .

We also obtained high-precision (0.08% rms) relative photometry of Gl 581 during a potential transit of the 3-days Gl 581, which had a ~5% *a priori* geometric transit probability. At a 4 σ confidence level, those observations exclude transits by a realistically dense Gl 581e for transit centers between -1 and +2.3 σ of the date predicted by our ephemeris. Gl 581e is thus unlikely to transit, though wider coverage of the transit window would be needed to fully exclude that it does.

Acknowledgements. We would like to thank the ESO La Silla staff for their excellent support, and our collaborators of the HARPS consortium for making this instrument such a success, as well as for helping obtain well sampled observations through observing time exchange.

Some of the reported observations were made with the INT operated on the island of La Palma by the Isaac Newton Group in the Spanish Observatorio del Roque de Los Muchachos of the Instituto de Astrofísica de Canarias.

NCS acknowledges the support by the European Research Council/European Community under the FP7 through Starting Grant agreement number 239953, as well as the support from Fundação para a Ciência e a Tecnologia (FCT) through program Ciência2007 funded by FCT/MCTES (Portugal) and POPH/FSE (EC), and in the form of grants reference PTDC/CTE-AST/098528/2008 and PTDC/CTE-AST/098604/2008.

MR acknowledges support from ALMA-CONICYT projects 31090015 and 31080021.

References

- Andrae, R., Schulze-Hartung, T., & Melchior, P. 2010, ArXiv e-prints
 Anglada-Escudé, G. & Dawson, R. I. 2010, ArXiv e-prints
 Bonfils, X., Delfosse, X., Udry, S., et al. 2005a, A&A, 442, 635
 Bonfils, X., Forveille, T., Delfosse, X., et al. 2005b, A&A, 443, L15
 Bouchy, F., Pepe, F., & Queloz, D. 2001, A&A, 374, 733
 Delfosse, X., Forveille, T., Mayor, M., et al. 1998, A&A, 338, L67
 Gilliland, R. L., Brown, T. M., Kjeldsen, H., et al. 1993, AJ, 106, 2441
 Gregory, P. C. 2011, MNRAS, 856
 Hawley, S. L., Gizis, J. E., & Reid, I. N. 1996, AJ, 112, 2799
 Heng, K. & Vogt, S. S. 2011, MNRAS, 738
 Johnson, J. A., Winn, J. N., Cabrera, N. E., & Carter, J. A. 2009, ApJ, 692, L100
 Leggett, S. K. 1992, ApJS, 82, 351
 Lovis, C., Mayor, M., Pepe, F., et al. 2006, Nature, 441, 305
 Lovis, C. & Pepe, F. 2007, A&A, 468, 1115
 Mayor, M., Pepe, F., Queloz, D., et al. 2003, The Messenger, 114, 20
 Mayor, M., Udry, S., Lovis, C., et al. 2009, A&A, 493, 639
 Mermilliod, J.-C., Mermilliod, M., & Hauck, B. 1997, A&AS, 124, 349
 Pepe, F., Lovis, C., & Ségransan, D. e. a. 2011, in The Astrophysics of planetary systems - formation, structure, and dynamical evolution (IAU Symposium 276), in press, ed. L. Arnold, F. Bouchy, & C. Moutou
 Pierrehumbert, R. T. 2011, ApJ, 726, L8+
 Press, W. H., Teukolsky, S. A., Vetterling, W. T., & Flannery, B. P. 1992, Numerical recipes in FORTRAN. The art of scientific computing (Cambridge: University Press, —c1992, 2nd ed.)
 Schlafman, K. C. & Laughlin, G. 2010, ArXiv e-prints
 Selsis, F., Kasting, J. F., Levrard, B., et al. 2007, A&A, 476, 1373
 Tuomi, M. 2011, A&A, 528, L5+
 Udry, S., Bonfils, X., Delfosse, X., et al. 2007, A&A, 469, L43

- van Leeuwen, F., ed. 2007, Astrophysics and Space Science Library, Vol. 350, Hipparcos, the New Reduction of the Raw Data
 Vogt, S. S., Butler, R. P., Rivera, E. J., et al. 2010, ApJ, 723, 954
 von Bloh, W., Cuntz, M., Franck, S., & Bounama, C. 2011, A&A, 528, A133+
 Walton, N. A., Lennon, D. J., Greimel, R., et al. 2001, The Newsletter of the Isaac Newton Group of Telescopes, 4, 7
 Wordsworth, R. D., Forget, F., Selsis, F., et al. 2011, ApJ, 733, L48+

Table 3. Radial-velocity measurements and error bars for Gl 581. All velocities are relative to the solar system barycenter, and corrected from the 0.20 [m s⁻¹] perspective acceleration computed from the Hipparcos parallax and proper motion. Only available electronically.

JD-2400000	S/N	RV [km s ⁻¹]	Uncertainty [km s ⁻¹]
53152.71289	48.8	-9.2163	0.0011
53158.66346	41.0	-9.2251	0.0013
53511.77334	42.8	-9.2133	0.0012
53520.74475	38.3	-9.1957	0.0014
53573.51204	39.2	-9.2054	0.0013
53574.52233	46.0	-9.1970	0.0011
53575.48075	55.3	-9.2017	0.0010
53576.53605	53.0	-9.2132	0.0010
53577.59260	43.0	-9.2169	0.0012
53578.51071	62.5	-9.2057	0.0009
53578.62960	45.0	-9.2038	0.0011
53579.46256	57.8	-9.1928	0.0009
53579.62105	49.2	-9.1913	0.0011
53585.46177	43.9	-9.1983	0.0011
53586.46516	66.2	-9.2091	0.0008
53587.46470	30.6	-9.2233	0.0016
53588.53806	19.4	-9.2142	0.0026
53589.46202	66.7	-9.2000	0.0008
53590.46390	59.7	-9.1933	0.0008
53591.46648	64.0	-9.1983	0.0008
53592.46481	61.5	-9.2113	0.0008
53606.55168	24.2	-9.1912	0.0021
53607.50753	52.8	-9.1945	0.0010
53608.48264	42.7	-9.2098	0.0012
53609.48845	32.1	-9.2174	0.0016
53757.87732	52.3	-9.2003	0.0010
53760.87548	38.9	-9.2075	0.0013
53761.85922	37.0	-9.1986	0.0014
53811.84694	40.3	-9.1996	0.0013
53813.82702	60.7	-9.2160	0.0009
53830.83696	56.9	-9.2078	0.0009
53862.70144	57.6	-9.2066	0.0009
53864.71366	49.1	-9.1922	0.0011
53867.75217	48.2	-9.2153	0.0011
53870.69660	48.4	-9.1997	0.0011
53882.65776	57.9	-9.2174	0.0009
53887.69074	66.0	-9.2117	0.0008
53918.62175	45.9	-9.1983	0.0011
53920.59495	50.7	-9.2245	0.0010
53945.54312	51.4	-9.1968	0.0010
53951.48593	66.4	-9.1995	0.0008
53975.47160	54.9	-9.2134	0.0010
53979.54398	41.4	-9.2134	0.0013
54166.87418	46.3	-9.2189	0.0011
54170.85396	62.1	-9.1981	0.0009
54194.87235	48.4	-9.2185	0.0011
54196.75038	43.1	-9.1897	0.0012
54197.84504	41.9	-9.1908	0.0012
54198.85551	40.6	-9.2082	0.0013
54199.73287	54.7	-9.2114	0.0010
54200.91092	49.5	-9.2061	0.0011
54201.86855	52.6	-9.1967	0.0010
54202.88260	53.2	-9.1935	0.0010
54228.74156	47.9	-9.1975	0.0011
54229.70048	33.2	-9.1957	0.0015
54230.76214	51.8	-9.2078	0.0010
54234.64592	45.1	-9.1914	0.0012
54253.63317	50.9	-9.2154	0.0010
54254.66481	54.5	-9.2104	0.0010
54291.56885	36.7	-9.2129	0.0014
54292.59081	62.0	-9.2058	0.0009
54293.62587	56.6	-9.1962	0.0010
54295.63945	46.3	-9.2164	0.0011
54296.60611	40.6	-9.2257	0.0013
54297.64194	53.7	-9.2143	0.0010
54298.56760	47.8	-9.1983	0.0011
54299.62220	31.5	-9.1951	0.0016
54300.61911	52.4	-9.2070	0.0010
54315.50749	30.5	-9.1920	0.0017
54317.48085	56.2	-9.2130	0.0010
54319.49053	37.8	-9.2031	0.0014

Table 5. Relative photometry of Gl 581 during the potential May 17th transit of Gl 581e, before correction of the slow drifts by a polynomial. Only available electronically.

JD-2400000	r'
54969.43393	1.003231
54969.43457	1.001711
54969.43522	1.002289
54969.43585	1.000873
54969.43649	1.001837
54969.43713	1.001473
54969.43776	1.001896
54969.43841	1.000586
54969.43905	1.001324
54969.43969	1.002118
54969.44032	1.001365
54969.44095	1.002456
54969.44160	1.001024
54969.44223	1.002106
54969.44288	1.000896
54969.44352	1.000395
54969.44415	1.001685
54969.44479	1.002107
54969.44543	1.000877
54969.44606	1.002166
54969.44671	0.998851
54969.44735	1.000762
54969.44798	1.002343
54969.44862	1.002358
54969.44925	1.000580
54969.44989	1.002454
54969.45054	1.001147
54969.45118	1.000453
54969.45183	1.000730
54969.45246	1.001324
54969.45310	1.002008
54969.45372	1.000541
54969.45437	1.000782
54969.45501	1.001169
54969.45565	0.999198
54969.45629	1.000649
54969.45692	1.000302
54969.45757	1.000450
54969.45820	1.000557
54969.45884	1.000211
54969.45949	1.000808
54969.46013	1.000459
54969.46076	1.001742
54969.46140	1.001292
54969.46205	1.001665
54969.46268	1.001565
54969.46331	0.999238
54969.46396	1.000638
54969.46460	0.999178
54969.46524	1.001544
54969.46588	1.001292
54969.46651	0.999200
54969.46715	0.999394
54969.46780	0.999992
54969.46845	0.998215
54969.46908	1.001774
54969.46972	1.001082
54969.47036	1.001217
54969.47099	1.000355
54969.47164	1.000418
54969.47228	1.001288
54969.47291	0.999573
54969.47355	1.000552
54969.47419	0.998711
54969.47484	1.001283
54969.47547	0.999626
54969.47612	1.001408
54969.47675	0.999846
54969.47739	1.000445
54969.47803	1.000111
54969.47868	0.998621
54969.47932	0.999706
54969.47995	0.999958
54969.48058	0.999913